Evaluation of a phase change solvent for CO_2 capture: Absorption and desorption tests

Diego D. D. Pinto, Syed A. H. Zaidy, Ardi Hartono, Hallvard F. Svendsen*

Department of Chemical Engineering, Norwegian University of Science and Technology, N-7491 Trondheim, Norway

Abstract

A blend of a tertiary amine (DEEA) and a diamine (MAPA) was studied in a screening apparatus for preliminary absorption tests. Two immiscible liquid phases were formed upon CO_2 loading and the system was shown to have large capacity for CO_2. The two phases were analyzed individually for both amines and CO_2. MAPA and water were found concentrated in the heavy CO_2 rich phase whereas the CO_2 lean phase contained mainly of DEEA. Volumetric phase ratio was measured as function of CO_2 loading and together with the individual phase compositions this forms part of a basis for an equilibrium model. The CO_2 rich phase was heated to desorption temperatures and shown to regenerate CO_2 at higher pressures than normally used for 30 wt.% MEA. The data enabled understanding the system behavior as MAPA is first loaded in the heavy phase and subsequently DEEA reacts with CO_2 and dissolves. The data show that the system has potential for significant reduction in regeneration heat through high cyclic capacity, very high CO_2 stripping pressures, and for operating where the heat of reaction lies between primary and tertiary amines. The tests also give good estimates for the absorption rate at higher loadings.

Keywords: Screening, phase change solvent, DEEA, MAPA, CO_2 Capture

*Corresponding author

Address: Sem Slands vei 6, Department of Chemical Engineering, Norwegian University of Science and Technology 7491 Trondheim - Norway

Email address: hallvard.svendsen@chemeng.ntnu.no (Hallvard F. Svendsen)

1. Introduction

Reduction of carbon dioxide emissions is still a very important topic and the research on reducing cost and energy demand for its capture has increased over the past years. Using energy efficiently, reducing energy waste, changing fuel sources to alternative sources poorer in carbon content and carbon capture and storage (CCS) are some ways of reducing the CO_2 emissions. Among the CCS technologies, chemical absorption using aqueous amine solutions with thermal regeneration of the solvent is the most developed and applied technology for CO_2 capture (Svendsen et al., 2011). The 30 mass % monoethanolamine (MEA) system is the benchmark solvent for this technology (Aroonwilas & Veawab, 2009; Rey et al., 2013) and research on this solvent is still progressing (see, for example, Razi et al., 2013; Vevelstad et al., 2013).

Most of the energy required for CO_2 capture in amine scrubbing systems is used for regenerating the solvent (Aroonwilas & Veawab, 2007). Process modifications are used in an attempt to reduce this demand. Several process modifications were studied and proposed in the literature (Cousins et al., 2011a,b; Karimi et al., 2011; Oyenekan & Rochelle, 2007; Rochelle et al., 2011). Nevertheless, the development of new solvents or solvent blends is an important way of reducing the energy demand in amine scrubbing plants. Apart from MEA, piperazine (PZ) and piperazine blends, AMP(2-amino-2-methyl-1-propanol) based systems, for instance with PZ, and amino acid based systems have been intensively studied (Jockenhvel & Schneider, 2011; Kuettel et al., 2013). Dugas & Rochelle (2009), for instance, showed that the 8 m piperazine solution has 75% higher capacity than a 7 m MEA solution. Also, CO_2 reaction rates are 2-3 times faster on PZ solutions. Other examples are large scale tests with commercial solvents which are claimed to be better than aqueous solutions of MEA, as the Cansolv solvent and KS-1 from MHI, (see Endo et al., 2011; Just, 2013; Kamijo et al., 2013; Shaw, 2009).

A new breed of systems, the phase change solvents, has received much attention during the last 4-5 years. Precipitating systems with amino acid salts

(Ma'mun & Kim, 2013; Sanchez-Fernandez et al., 2013) and carbonated solutions (Moene et al., 2013) are claimed to be promising systems for CO_2 capture. IFPEN recently proposed the DMX^{TM}process in which the solvent forms two immiscible liquid phases upon CO_2 loading (Aleixo et al., 2011; Raynal et al., 2011a,b). This process is able to operate with energy demands as low as 2.1 GJ/ton of CO_2. Other amine based solvents that form two phases before or after CO_2 loading were recently patented (Svendsen & Trollebø, 2013).

The development of a new solvent is not simple. A large set of experiments must be performed in order to characterize the system. Screening experiments is a fast way to identify potential solvents for CO_2 capture, e.g. Ma'mun et al. (2007) used a screening apparatus to evaluate the absorption rate of different amine based solvents for CO_2 capture. Aronu et al. (2009) modified the same apparatus to allow for desorption operation testing. The authors presented a comparison of absorption and stripping performance for some amine/amine blend solutions. Aronu et al. (2010) and Aronu et al. (2011) used the screening apparatus to evaluate amino acid salts and amine/amine blend solvents, respectively.

In this work, a blend of 5M DEEA (Diethylethanolamine) and 2M MAPA (N-Methyl-1,3-diaminopropane) was tested in the screening apparatus. This mixture, as in the DMX^{TM}solvent, forms two liquid phases upon CO_2 loading. By separating out the CO_2 rich phase, it is possible to send a smaller volume of solvent for regeneration, thereby, potentially reducing the process energy demand. Also, the CO_2-rich phase can have a potential for easy stripping, thereby also reducing the stripping steam demand and possibly increasing the regeneration pressure. The amines here studied are potential solvents for CO_2 capture, and were also studied by other authors (Hartono et al., 2013; Monteiro et al., 2013b,a; Pinto et al., 2014; Voice et al., 2013). The screening apparatus used in Aronu et al. (2010) was used for absorption tests at different CO_2 partial pressures and temperatures. The system was characterized by individual analyses of the two liquid phases at equilibrium, and the phase ratio recorded. The CO_2-rich phase formed upon CO_2 loading was separated after absorption

3

⁸⁷ and used for desorption tests in a separate apparatus which is also shown in this
⁸⁸ work.

2. The phase change solvent

⁹⁰   As in the DMX^{TM}process (Raynal et al., 2011a), the system studied here
⁹¹ forms two phases upon CO_2 loading. The chemicals used on the DMX^{TM}process
⁹² are not given anywhere. In this work, an aqueous solution of a tertiary alka-
⁹³ nolamine (DEEA) and a diamine (MAPA) with a primary and a secondary
⁹⁴ amine group was studied. In Fig. 1 the chemical structure of the amines used
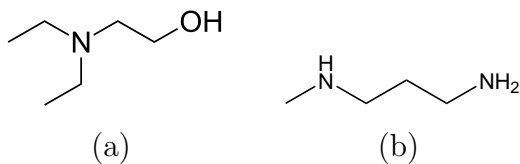⁹⁵ in the solution is shown.

Figure 1: Chemical structure: (a) DEEA; (a) MAPA.

⁹⁶   The system has an advantage of combining high absorption rate, provided
⁹⁷ by the diamine, and high capacity from the tertiary amine. Puxty et al. (2009)
⁹⁸ showed that DEEA has a significant absorption capacity while MAPA has a high
⁹⁹ initial absorption rate. Moreover, the energy required for regenerating a tertiary
¹⁰⁰ amine is lower than for primary and secondary amines (Kim & Svendsen, 2011).
¹⁰¹ It is therefore a potential for lowering the total energy consumption of the overall
¹⁰² process significantly.

¹⁰³   A solution of 5M DEEA and 2M MAPA is a single phase solution. When the
¹⁰⁴ solution starts to absorb CO_2, at some point, it becomes turbid which indicates
¹⁰⁵ a phase changing behaviour. After leaving the loaded solution to rest two clear
¹⁰⁶ liquid phases can be observed. This behaviour is shown in Fig. 2.

2.1. The phase change solvent capture process

¹⁰⁸   The phase change solvent uses the advantage of the phase split to reduce
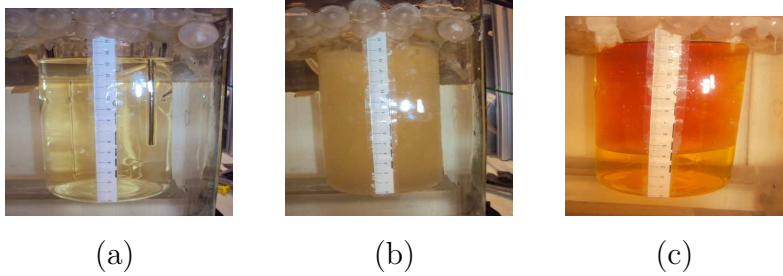¹⁰⁹ the energy demand of the CO_2 capture process. The changes in the process

Figure 2: A 5M DEEA/2M MAPA solution: (a) Before, (b) During and (c) after CO_2 loading.

configuration, as shown in Fig. 3, are made not only to reduce the energy demand, but also as a result of the characteristics of the system. The process flow diagram presented in this work is very similar to the one presented in Raynal et al. (2011b). However, the phase separator is placed before the cross heat exchanger.
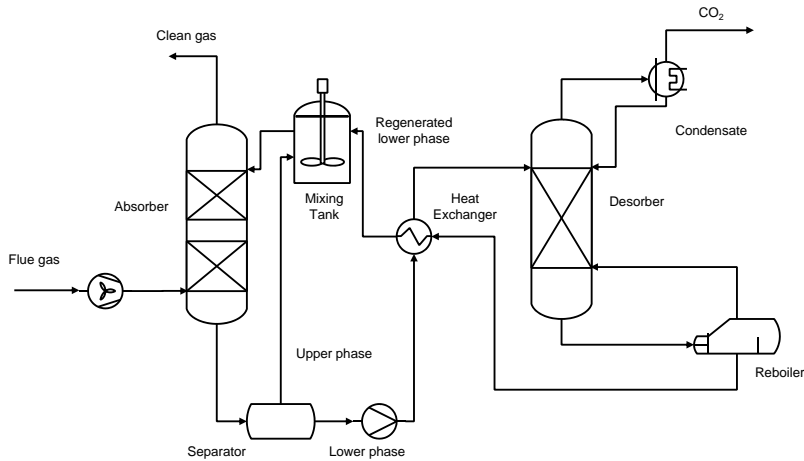

Figure 3: Capture process layout for the phase change solvent

3. Experiments

The apparatus' descriptions and their operational details are given in this section.

3.1. Screening apparatus

¹¹⁹ The screening apparatus (Fig. 4) is designed to operate up to 80°C and at

¹²⁰ atmospheric conditions for rapid evaluation of absorption and stripping perfor-

¹²¹ mance of solvents. As discussed in Aronu et al. (2009) and Ma'mun et al. (2007),

¹²² the results from the screening apparatus are semi quantitative and should be

¹²³ understood only as an indication of a solvent's performance. The apparatus

¹²⁴ used in this work is the same as the one used in Aronu et al. (2010) with minor

¹²⁵ modifications. The reactor was changed to a glass volume graded vessel where

¹²⁶ it was possible to see the phase change formation and the CO_2 analyzer was

¹²⁷ also replaced by a Rosemount BINOS 100 IR CO_2-analyzer.
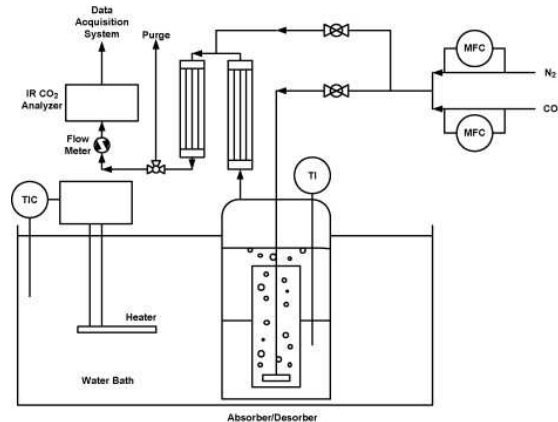

Figure 4: Simplified diagram of the screening apparatus (Aronu et al., 2010).

¹²⁸ A known volume and mass (around 750 ml) of the solvent was weighed into

¹²⁹ the reactor and a synthetic mixture of CO_2 and N_2, with a total flow of 5

¹³⁰ Nl/min, was bubbled into the solvent. The CO_2 concentration (flow) in the

¹³¹ inlet gas was adjusted to the desirable value by adjusting the mass flow of N_2

¹³² and CO_2 while keeping the total flow at 5 Nl/min. After bubbling through the

¹³³ solution, the gas stream was cooled on-line through two condensers placed on

¹³⁴ top of each other and the condensate was directly returned to the reactor. The

¹³⁵ dried gas was sent to the IR analyzer for CO_2 analysis.

¹³⁶ The absorption tests were performed at 40, 60 and 80°C and from 1 to

20 kPa of CO_2 partial pressure in the inlet gas. An experiment was stopped when 95% of the concentration of the inlet gas was achieved in the outlet of the reactor. The mixture was then left to rest so that the phases could separate at the experimental temperature. The volumes of the lower and upper phases were recorded and sampled individually at the experimental temperature, after which they were separated and stored in different bottles for further analysis.

3.2. High pressure desorption apparatus

Stripping experiments were done on the lower phase (CO_2 rich phase) generated in the screening apparatus. A different apparatus was used for this purpose. The apparatus consisted of a 150 ml stainless steel vessel immersed in an oil bath where the temperature was held constant by a Julabo 6 heating system. A thermocouple was placed inside the vessel and in contact with the liquid (Fig. 5). The temperature of the liquid as well as the pressure of the system were read and recorded through a program coded in LabView software. The cylinder was evacuated to about 20 mbar and around 80 ml of a lower phase sample was sucked in. The oil bath was set to a desired temperature, and once the temperature and pressure were stable, a point was recorded. Temperature and pressure were considered stable if in a 10 minutes window no variations occurred above a given limit ($\pm$ 0.1°C and $\pm$ 1 mbar). The temperature was then increased and the procedure was repeated until the pressure was close to 6 bar. This was due to the pressure transducer having an upper limit of 6 bar.

A total of eight samples from the screening tests were tested for high pressure desorption. Table 1 shows the samples selected for the high pressure desorption tests.

4. Results

4.1. Screening calculations

A Labview data acquisition software was used to record the measured variables (temperatures, flows and CO_2 content in the outlet gas) every minute from
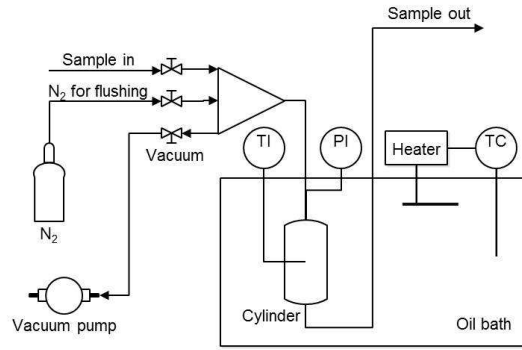
Figure 5: Simplified diagram of the high pressure desorption apparatus.

Table 1: Screening samples taken for high pressure desorption tests

Sample	Absorption Temperature $[^\circ C]$	P_{CO_2}
1	40	6
2	40	8
3	40	10
4	40	13
5	60	8
6	60	10
7	60	13
8	80	8

165 the start of the experiment. The flows of dry N_2 and CO_2 in the inlet gas were

166 adjusted to the desirable concentration and were kept constant throughout the

167 experiment. The dry N_2 gas flow was considered to be the same in the inlet and

168 outlet since N_2 is an inert gas. The total molar flow could then be calculated

169 from the N_2 inlet flow and the CO_2 content given by the IR analyzer, as shown

170 by Eq. 1. The CO_2 mole fraction in the outlet gas stream was calculated by

171 Eq. 2. Finally, the amount of CO_2 absorbed is given by the difference between

172 amounts of CO_2 in the inlet and outlet, and can be calculated from the measured

173 variables according to Eq. 3.

$$Q_{total}^{out}[mol/min] = \frac{n_{N_2}^{in}}{x_{N_2}^{out}} = \frac{n_{N_2}^{in}}{(1 - x_{CO_2}^{out})} \tag{1}$$

$$x_{CO_2}^{out} = \frac{(CO_2 \text{ vol\%})}{100} \tag{2}$$

$$Q_{CO_2}[mol/min] = n_{CO_2}^{in} - n_{CO_2}^{out} = n_{CO_2}^{in} - x_{CO_2}^{out} Q_{total}^{out} \tag{3}$$

174 The CO_2 absorption rate was calculated according to Eq. 4. Since the mass

175 (M^{sol}) and the volume (V) of the solvent in the reactor and the accumulated

176 amount of CO_2 ($Q_{CO_2}^{Acc.}$) are known, the loading in moles of CO_2 per kilogram

177 of solvent could be calculated according to Eq. 5. It is important to point it

178 out that Eq. 5 computes the loading with respect to the total solvent mass. In

179 other words, this accounts for the weight of both the lower and upper phases.

$$r_{CO_2} \left[\frac{mol}{kg.min}\right] = \frac{Q_{CO_2}}{M^{sol}} \tag{4}$$

$$\alpha \left[\frac{mol \ CO_2}{kg \ solution}\right] = \frac{Q_{CO_2}^{Acc.}}{M^{sol}} \tag{5}$$

180 *4.2. Screening results*

181 The absorption rates of CO_2 at 40, 60 and 80°C are shown in Fig. 6, 7 and

182 8, respectively. As reference a 5M MEA solution (30 % wt.) was tested at 40

183 °C and 10 kPa of CO_2 partial pressure.

9

The comparison between the DEEA/MAPA system and MEA is not straight forward. Several properties, for example, the viscosity, which is much higher in the DEEA/MAPA system, are different making the comparison difficult. Although the superficial gas velocity was the same for all experiments, the gas-liquid interfacial area could not be guaranteed to be the same, as explained before in Ma'mun et al. (2007). In Fig. 6, up to the region of 1.2 mol CO_2/kg solution loading, it is possible to conclude that the DEEA/MAPA system shows a slightly higher absorption rate than the 5M MEA (indicating that it absorbs CO_2 faster than the 5M MEA) and it retains the absorption rate more constant than 5M MEA. However, when approaching the equilibrium (high loading region) the MEA solution has a sharper fall towards zero absorption rate, while the DEEA/MAPA system presents a more drawn out tail type of ending. This is due to the saturation of the primary and secondary amine groups in MAPA while the tertiary amine (DEEA) is still absorbing but at lower absorption rates.

Increasing the temperature led to a small increase in the CO_2 absorption rate. Increasing the CO_2 partial pressure in the gas, also, increases the reaction rate, as shown in Fig. 9. This is already expected since the driving force is increase when the amount of CO_2 is increased in the gas. It should be noted, however, that the initial flat part of all the screening curves is not representative of the real absorption rates as in this region, all, or close to all, CO_2 in the gas is removed. However, in the tail end of the curves the measurements give good indication of the rate of absorption in the DEEA/MAPA system.

After an experiment was terminated (achieving 95% of the CO_2 concentration in the inlet gas stream in the outlet gas stream), the solvent was left to separate at the experiments temperature, so the volume ratios could be registered. The phase separation time was also recorded and it varied from 25-30 minutes at 40°C to 3-5 minutes at 80°C.

Even though the rate measurements are only semi-quantitative, the screening experiments contribute with many other measurements which can be used in understanding and modeling of the system. The volume ratio (ϕ), defined as the ratio between the volumes of the lower and the upper phase, and the final
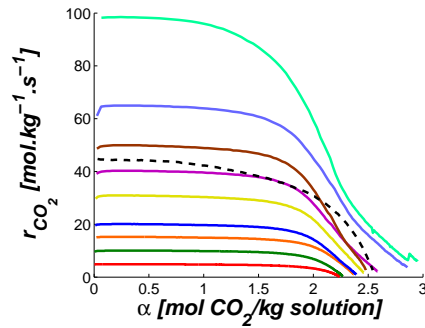
Figure 6: Screening tests performed at 40°C. Solid curves from bottom to top: 1, 2, 3, 4, 6, 8, 10, 13 and 20 kPa P_{CO_2}. Dashed curve: 30 mass% MEA at 10 kPa P_{CO_2}.
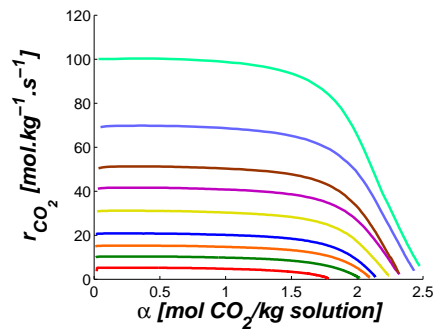

Figure 7: Screening tests performed at 60°C. Solid curves from bottom to top: 1, 2, 3, 4, 6, 8, 10, 13 and 20 kPa P_{CO_2}.
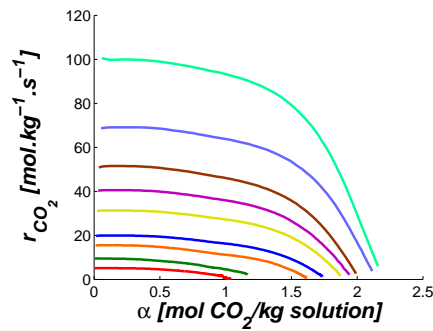

Figure 8: Screening tests performed at 80°C. Solid curves from bottom to top: 1, 2, 3, 4, 6, 8, 10, 13 and 20 kPa P_{CO_2}.
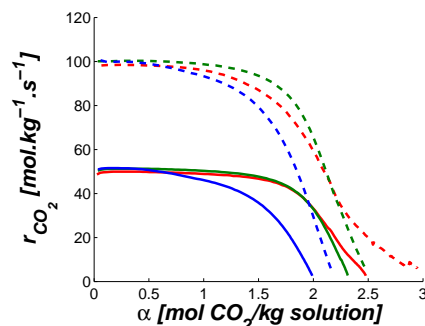
11

Figure 9: Screening tests performed at 10 kPa and: (—) $40°C$, (—) $60°C$ and (—) $80°C$. Screening tests performed at 20 kPa and: (- -) $40°C$, (- -) $60°C$ and (- -) $80°C$

loading (α_{final}), in mol CO_2/ kg of solution, are given in Table A1 in the appendix.

Both the upper and lower phases were analyzed for CO_2 and amine content. LCMS analyses were used to quantify the ratio between the concentrations of DEEA and MAPA while total alkalinity and CO_2 content analyses were performed by the procedure described in Monteiro et al. (2013a). With the concentration ratio, the total alkalinity and the CO_2 content, the individual species concentrations were calculated for all samples and are shown in Table A2 in the appendix.

From the analyses it was possible to identify a CO_2 rich phase (the lower phase) and a CO_2 lean phase (the upper phase). The CO_2 rich phase was rich in MAPA and H_2O whereas the CO_2 lean phase was composed mainly of DEEA. The upper phase would work as a buffer of DEEA, which would move to the lower phase as more CO_2 is capture by the solvent.

The concentration ratios between DEEA and MAPA (mole/mole) in the lower phase given by the LCMS are shown in Fig. 10. Apart from some points at low CO_2 concentration at $80°C$, the concentration of DEEA in the lower phase increases more or less linearly with the increase of CO_2 in the system and the slope of this linear tendency decreases with the increase of temperature. The 2-3 points at low CO_2 loading at $80°C$ are believed not to be outliers, but a result

12

of the increased miscibility between the two phases at higher temperatures. There was, however, no second experiment performed at 80°C for checking reproducibility. As temperature increases, the solubility of DEEA in the lower phase goes up and this is reflected in the increased DEEA concentration seen in these points. This is also shown in Fig. 11 where the volume ratio (ϕ), between the lower and upper phase is given as function of CO_2 partial pressure and temperature. At 40°C the lower/upper ratio increases with loading in an almost linear fashion. At 60°C the ratio increases rapidly at low partial pressures, and loadings, whereas it levels off at higher loadings. At 80°C this tendency is even clearer as the lower/upper ratio is very low at low loading, indicating better miscibility. This supports the previously discussed results shown in Fig. 10 at 80°C. Although the measurements show clear trends for the volume ratios of the phases, the uncertainty in the measurements is relatively high and estimated to ±0.03-0.05 in volume ratio.
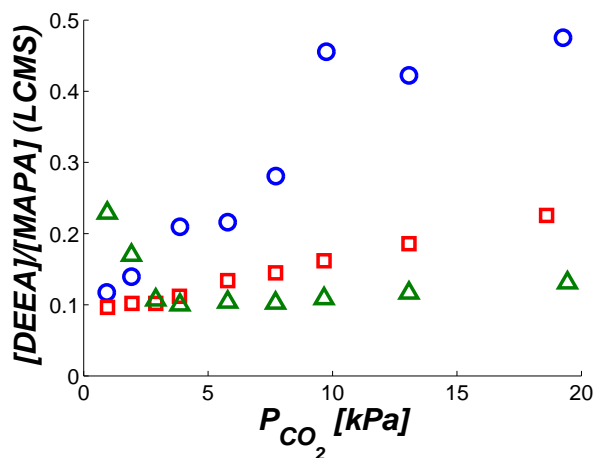

Figure 10: Concentration ratio (mole DEEA/ mole MAPA) from LCMS in the lower phase. Experiments performed at: (○) 40, (□) 60 and (△) 80°C.

The mole fractions of the species are shown in Fig. 12, 13 and 14 for the experiments performed at 40, 60 and 80°C respectively. As previously mentioned, it is possible to identify a CO_2 rich (lower) and lean (upper) phase. The DEEA
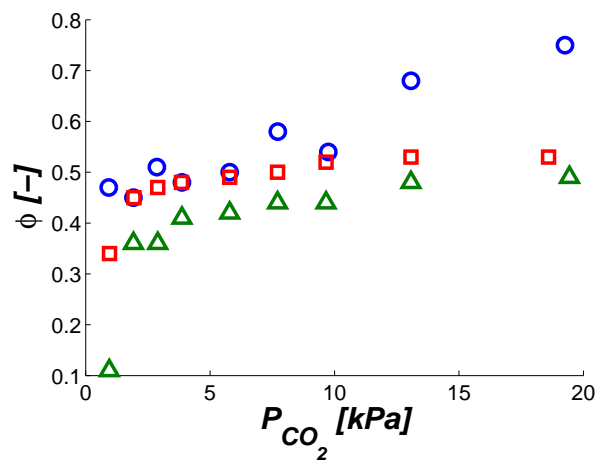
13

Figure 11: Volume distribution. Experiments performed at: ($\circ$) 40, ($\square$) 60 and ($\triangle$) 80°C.

is mainly concentrated in the upper phase. However, as more CO_2 is added to the system, the DEEA tends to migrate to the lower phase and, therefore, its concentration is reduced in the upper phase.

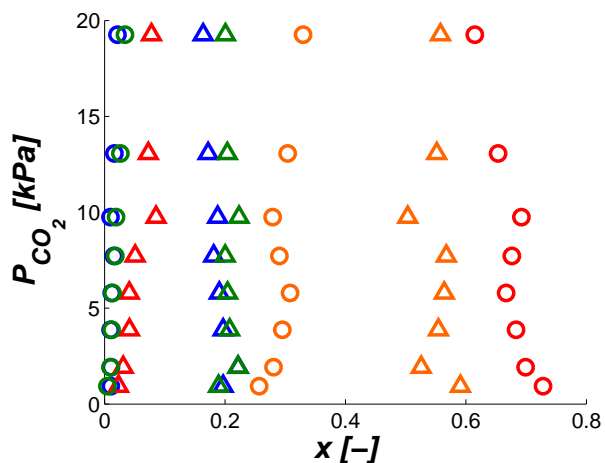Figure 12: : Mole fraction distribution for experiments taken at 40°C. Symbols for the upper phase: ($\circ$) MAPA, ($\circ$) DEEA, ($\circ$) CO_2 and ($\circ$) H_2O. Symbols for the lower phase: ($\triangle$) MAPA, ($\triangle$) DEEA, ($\triangle$) CO_2 and ($\triangle$) H_2O.

Fig. 15 shows the CO_2 content (from titration) per kg solution for the lower

14

Figure 13: Mole fraction distribution for experiments taken at 60°C. Symbols for the upper phase: (○) MAPA, (○) DEEA, (○) CO_2 and (○) H_2O. Symbols for the lower phase: (△) MAPA, (△) DEEA, (△) CO_2 and (△) H_2O.
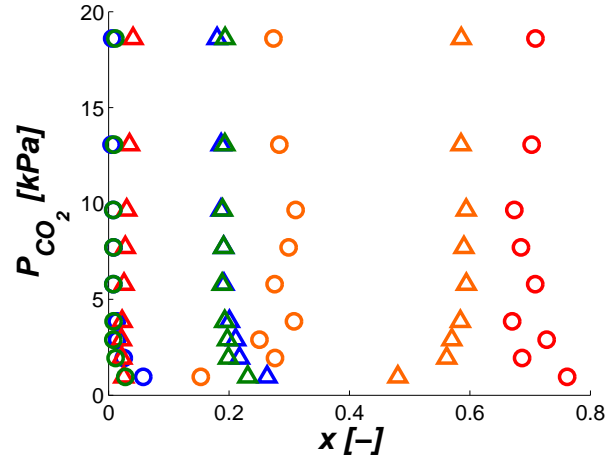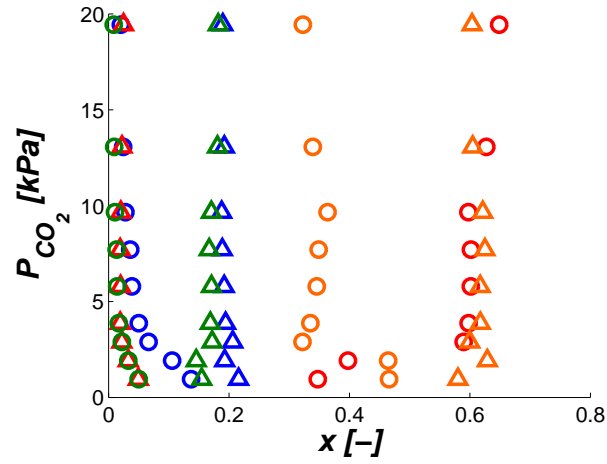

Figure 14: Mole fraction distribution for experiments taken at 80°C. Symbols for the upper phase: (○) MAPA, (○) DEEA, (○) CO_2 and (○) H_2O. Symbols for the lower phase: (△) MAPA, (△) DEEA, (△) CO_2 and (△) H_2O.

and upper phases as function of the absorption CO_2 partial pressure. The CO_2
content is nearly constant as function of the absorption CO_2 partial pressure,
except for the 2-3 first points. As more CO_2 is added to the system, more DEEA
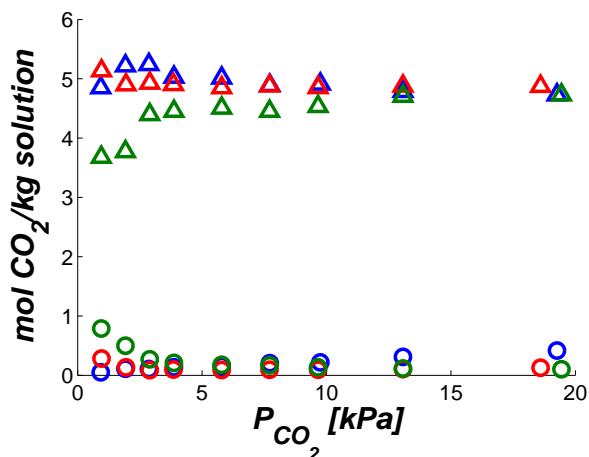migrates to the lower phase, thus, keeping the ratio mole CO_2/kg solution close
to constant.

Figure 15: CO_2 content in the lower and upper phases as function of absorption CO_2 partial pressure. Upper phase: (○) 40, (○) 60 and (○) 80°C. Lower phase: (△) 40, (△) 60 and (△) 80°C.

After separating the phases, the density of each phase was measured at 25°C
for all experiments. Apart from the measurements at 80°C and low CO_2 partial
pressures, it seems that there is no significant variation in the sample densities.
Fig. 16 shows the densities for the upper and lower phases as function of the
experimental CO_2 partial pressure and temperature. The density data for low
loadings at 80°C again show the increased miscibility at higher temperatures.
The data are given in Table A4 in the appendix.

4.3. High pressure desorption tests

The lower phase solutions from the various screening tests were tested for
stripping performance as described in section 3.2. The lower phase of the DEEA
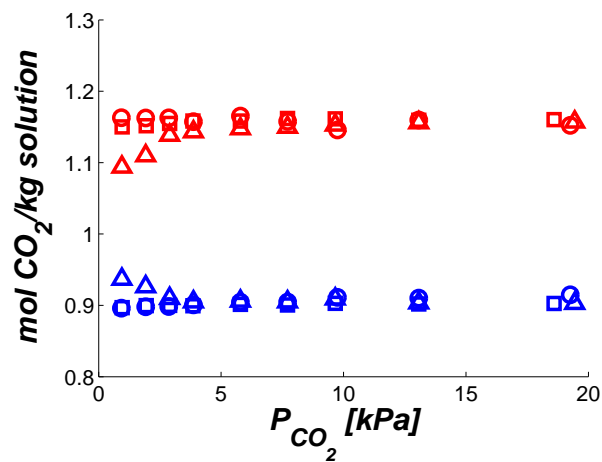
Figure 16: Densities of the phases at 25°C. Upper phase from experiments performed at: (○) 40, (□) 60 and (△) 80°C. Lower phase from experiments performed at: (○) 40, (□) 60 and (△) 80°C.

/MAPA system showed a high potential for generating CO_2 at elevated pressures.

Figure 17: Total pressure from lower phase samples with absorption taken at 40°C from the screening apparatus. P_{CO_2}: (△) 6 kPa, (○) 8 kPa, (◇) 10 kPa and (□) 13 kPa. (——) MEA at loading 0.5 mol CO_2/mol MEA (model from Hessen et al. (2010)).

17

In Fig. 17 are shown the vapor pressures of the lower phase, from absorption tests at 40°C and different CO_2 partial pressures, as a function of temperature. As expected, the total pressure increases with the sample CO_2 loading, reflected in the partial press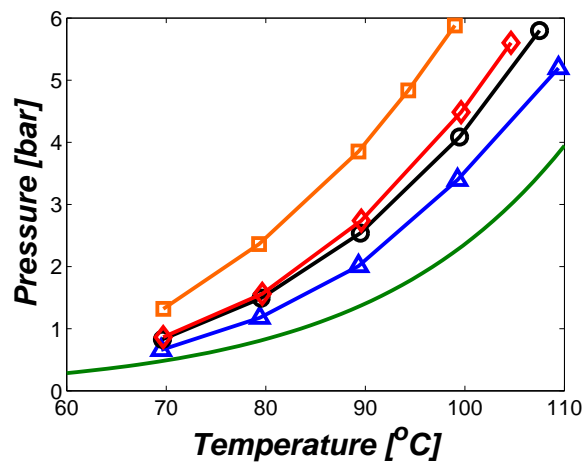ure at which it has been generated. It should be kept in mind that the solutions were generated at 95% of the given pressure. As can be seen the pressures that can be generated are significantly higher than for a representative 30 mass% MEA solution with loading 0.5 mole CO_2/mole MEA. The high pressures that can be obtained can be exploited in two ways. One way is to use a normal regeneration temperature of about 120°C and produce CO_2 at elevated pressure, possibly at 6-8 bar. This method will save electrical energy for the recompression of CO_2 to transportation pressure (around 110 Bar). In a coal based power station typically recompression energy will be 25-30% of the total energy demand and thus significant savings can be achieved. A second option is to operate the regenerator at lower temperatures than normal, e.g. below 100°C. By doing this the stripping pressure will not be increased compared to the normal situation but the quality of the heat to be supplied will be reduced. In some cases this may be a better option. A lower regeneration temperature will also positively affect the solvent degradation processes as these will be slowed down. The reason for the ease of stripping from this system is a result of the behavior of the blended system. As observed, the diamine MAPA is very rapidly loaded. This is seen from the flat part of the screening curves in Fig. 6-8. When MAPA is almost fully loaded, DEEA starts loading up and is transferred to the heavy bottom phase. When stripping it is basically DEEA that strips and the loading of MAPA remains nearly unchanged. This mechanism has another advantage. As shown by Arshad et al. (2013), the heat of absorption goes significantly down when MAPA is almost fully saturated and DEEA is being loaded. The heat of absorption drops from about 85-90 kJ/mole CO_2 in the range where MAPA loads to about 60 kJ/mole CO_2 when DEEA predominantly loads. The operational cycle in this system will be in this intermediate range where the heat of absorption and desorption will be determined mainly by DEEA, but also to some extent by MAPA. All the high

18

pressure desorption test results are displayed in Table A3.

5. Conclusions

Preliminary absorption tests made on a phase change solvent, composed of an aqueous mixture of 5M DEEA and 2M MAPA, were performed. The solvent showed a great absorption capacity. Upon CO_2 loading, the solvent splits in two immiscible phases. From the analyses it was possible to see that the CO_2 rich phase was rich in MAPA and H_2O whereas the CO_2 poor phase was mainly composed of DEEA. As more CO_2 was added to the system, more DEEA is transferred to the lower phase. The volume of the lower phase was also increased by adding more CO_2 to the system. The phase separation was accelerated by increasing the temperature.

Desorption tests made on the CO_2 rich phase from the screening tests showed that the DEEA/MAPA system can produce CO_2 at elevated pressures with the solvent regeneration performed at lower temperatures compared to the traditional 30 mass% MEA process.

The new, biphasic system will thus have three advantages. The cyclic capacity is high thereby reducing the sensible heat demand; the lower phase shows a significant potential for increased CO_2 pressure during stripping thus enabling regeneration at elevated pressure or lower temperature, and finally the operation will take place in a domain where mainly loading and stripping of the tertiary amine takes place, thereby lowering the heat of absorption.

The data generated are of great value for further modeling purposes. Nonetheless, more experiments need to be carried out to confirm the systems potential as a solvent for CO_2 capture.

19

Appendix A: Experimental data

Table A1: DEEA/MAPA system volume ratio and final loading at different temperatures and P_{CO_2}

40 °C			60 °C			80 °C		
P_{CO_2} [kPa]	ϕ	α_{final} [mol/kg]	P_{CO_2} [kPa]	ϕ	α_{final} [mol/kg]	P_{CO_2} [kPa]	ϕ	α_{final} [mol/kg]
0.93	0.47	2.2347	0.96	0.34	1.7786	0.95	0.11	1.0368
1.92	0.45	2.2636	1.94	0.45	2.0180	1.92	0.36	1.1682
2.86	0.51	2.3675	2.90	0.47	2.0958	2.90	0.36	1.6157
3.87	0.48	2.3906	3.85	0.48	2.1380	3.87	0.41	1.7372
5.79	0.50	2.4595	5.79	0.49	2.2407	5.79	0.42	1.8720
7.72	0.58	2.5849	7.71	0.50	2.3207	7.71	0.44	1.9409
9.75	0.54	2.4792	9.66	0.52	2.3141	9.66	0.44	1.9901
13.07	0.68	2.8579	13.07	0.53	2.4329	13.07	0.48	2.1142
19.26	0.75	2.9505	18.6	0.53	2.4753	19.44	0.49	2.1587

Table A2: Individual species concentration (mol/l) for the upper
and lower phases after phase separation.

Absorption taken at 40°C								
P_{CO_2} [kPa]	0.93	1.92	2.86	3.87	5.79	7.72	9.75	13.07	19.26
Upper phase									
MAPA	0.1036	0.1073	N/A	0.1043	0.126	0.1631	0.1016	0.1747	0.2421
DEEA	7.1625	7.1071	N/A	7.0916	7.0686	7.0616	7.1797	7.0264	6.9115
CO_2	0.0460	0.1000	N/A	0.1211	0.1412	0.1861	0.1988	0.2826	0.3826
H_2O	2.5246	2.8536	N/A	3.0625	3.2645	3.0329	2.895	3.2692	3.7069
Lower phase									
MAPA	5.8666	6.0861	N/A	5.5173	5.4462	5.1229	4.7332	4.6847	4.4476
DEEA	0.6882	0.8489	N/A	1.1560	1.1761	1.4384	2.1558	1.9786	2.1137
CO_2	5.6418	6.0682	N/A	5.8192	5.8410	5.6590	5.6292	5.5524	5.4492
H_2O	17.6096	14.418	N/A	15.5282	16.1239	16.0315	12.6823	15.0301	15.1468
Absorption taken at 60°C									
P_{CO_2} [kPa]	0.96	1.94	2.9	3.85	5.79	7.71	9.66	13.07	18.6
Upper phase	0.5265	0.2572	0.1404	0.1430	0.0810	0.0862	0.0825	0.0508	0.0613
MAPA	6.9469	7.0057	7.1656	7.0374	7.1722	7.1121	7.1069	7.1783	7.1859

DEEA	0.2530	0.1200	0.0786	0.0887	0.0800	0.0833	0.0836	0.0938	0.1156
CO_2	1.3974	2.8197	2.4677	3.2325	2.7909	3.1043	3.2767	2.8973	2.7762
H_2O	0.5265	0.2572	0.1404	0.143	0.0810	0.0862	0.0825	0.0508	0.0613
Lower phase									
MAPA	6.7278	6.1633	6.0820	5.9125	5.7070	5.6784	5.5565	5.4773	5.2666
DEEA	0.6480	0.6275	0.6202	0.6617	0.7641	0.8228	0.8992	1.0175	1.1877
CO_2	5.9074	5.6423	5.6908	5.6793	5.6169	5.6718	5.6340	5.6551	5.6545
H_2O	12.282	15.9186	16.4308	17.1997	17.6921	17.5203	7.6773	17.1371	17.1123

Absorption taken at 80°C									
P_{CO_2} [kPa]	0.95	1.92	2.90	3.87	5.79	7.71	9.66	13.07	19.44
Upper phase									
MAPA	2.0265	1.4879	0.7399	0.5586	0.4338	0.4045	0.3218	0.2660	0.2178
DEEA	5.1342	5.6052	6.5639	6.6581	6.7498	6.7594	6.8310	6.8973	6.9735
CO2	0.7380	0.4630	0.2445	0.1890	0.1599	0.1516	0.1229	0.1047	0.0915
H2O	6.8850	6.5461	3.5844	3.7324	3.8779	3.9188	4.1590	3.7296	3.4692
Lower phase									
MAPA	5.6119	5.5516	5.9994	5.8536	5.818	5.7878	5.7497	5.7860	5.6992
DEEA	1.2844	0.9419	0.6417	0.5854	0.6042	0.5925	0.6253	0.6744	0.7453
CO2	4.0244	4.1857	5.0056	5.0913	5.1720	5.1214	5.2283	5.4405	5.4730

| H2O | 15.0900 | 18.0978 | 17.4517 | 18.5929 | 18.6896 | 19.1558 | 19.0301 | 18.1897 | 18.1393 |

Table A3: High pressure desorption data for the screening lower phase samples.

Screening experiment	Temperature [°C]	Pressure [mbar]
40°C and 6 kPa	69.50	656.479
	79.41	1174.313
	89.32	2007.091
	99.27	3394.332
	109.41	5193.126
40°C and 8 kPa	69.62	826.588
	79.53	1490.750
	89.51	2537.697
	99.47	4084.989
	107.50	5797.586
40°C and 10 kPa	69.70	863.062
	79.65	1559.486
	89.60	2738.535
	99.62	4484.843
	104.63	5602.400
40°C and 13 kPa	69.71	1318.472
	79.33	2361.130
	89.32	3850.758
	94.32	4834.645
	99.00	5879.321
60°C and 8 kPa	69.63	376.760
	79.57	655.999
	89.51	1119.848
	99.50	1940.140
	109.50	3195.233
	119.60	5105.616

60°C and 10 kPa	69.47	411.752
	79.51	669.675
	89.46	1201.867
	99.46	2056.919
	109.47	3365.524
	119.57	5383.384
60°C and 13 kPa	69.30	437.794
	79.33	776.192
	89.13	1363.450
	99.25	2243.332
	109.01	3648.222
	119.24	5606.304
80°C and 8 kPa	69.64	209.694
	74.60	270.101
	79.44	344.823
	89.40	589.248
	99.37	990.095
	109.42	1641.672
	119.50	2697.620

Table A4: Densities of the loaded and unloaded phases at 25°C.

Temperature [$°C$]	P_{CO_2}	ρ_{upper}	ρ_{lower}
	0.93	0.8960	1.1630
	1.92	0.8981	1.1625
	2.86	0.8984	1.1627
	3.87	0.9007	1.1574
40	5.79	0.9044	1.1652
	7.72	0.9047	1.1577
	9.75	0.9112	1.1458

	13.07	0.9101	1.1597
	19.26	0.9149	1.1522
	0.96	0.8968	1.1500
	1.94	0.8997	1.1516
	2.90	0.9000	1.1550
	3.85	0.8994	1.1582
60	5.79	0.9014	1.1582
	7.71	0.9006	1.1619
	9.66	0.9028	1.1613
	13.07	0.9020	1.1594
	18.60	0.9026	1.1603
	0.95	0.9367	1.0939
	1.92	0.9262	1.1097
	2.90	0.9097	1.1384
	3.87	0.9050	1.1433
80	5.79	0.9061	1.1476
	7.71	0.9050	1.1498
	9.66	0.9092	1.1527
	13.07	0.9035	1.1559
	19.44	0.9029	1.1571

References

Aleixo, M., Prigent, M., Gibert, A., Porcheron, F., Mokbel, I., Jose, J., & Jacquin, M. (2011). Physical and chemical properties of DMX^{TM} solvents. *Energy Procedia*, *4*, 148 – 155. URL: http://www.sciencedirect.com/science/article/pii/S1876610211000361. doi:http://dx.doi.org/10.1016/j.egypro.2011.01.035. 10th International Conference on Greenhouse Gas Control Technologies.

Aronu, U. E., Hoff, K. A., & Svendsen, H. F. (2011). CO$_2$ capture solvent

selection by combined absorptiondesorption analysis. *Chemical Engineering Research and Design*, *89*, 1197 – 1203. URL: http://www.sciencedirect. com/science/article/pii/S0263876211000335. doi:http://dx.doi.org/ 10.1016/j.cherd.2011.01.007. Special Issue on Distillation & Absorption.

Aronu, U. E., Svendsen, H. F., & Hoff, K. A. (2010). Investigation of amine amino acid salts for carbon dioxide absorption. *International Journal of Greenhouse Gas Control*, *4*, 771 – 775. URL: http://www.sciencedirect. com/science/article/pii/S1750583610000496. doi:http://dx.doi.org/ 10.1016/j.ijggc.2010.04.003.

Aronu, U. E., Svendsen, H. F., Hoff, K. A., & Juliussen, O. (2009). Solvent selection for carbon dioxide absorption. *Energy Procedia*, *1*, 1051 – 1057. URL: http://www.sciencedirect. com/science/article/pii/S1876610209001404. doi:http://dx.doi.org/ 10.1016/j.egypro.2009.01.139. Greenhouse Gas Control Technologies 9 Proceedings of the 9th International Conference on Greenhouse Gas Control Technologies (GHGT-9), 1620 November 2008, Washington DC, {USA}.

Aroonwilas, A., & Veawab, A. (2007). Integration of CO_2 capture unit using single- and blended-amines into supercritical coal-fired power plants: Implications for emission and energy management. *International Journal of Greenhouse Gas Control*, *1*, 143 – 150. URL: http://www.sciencedirect. com/science/article/pii/S1750583607000114. doi:http://dx.doi.org/ 10.1016/S1750-5836(07)00011-4. 8th International Conference on Greenhouse Gas Control Technologies GHGT-8.

Aroonwilas, A., & Veawab, A. (2009). Integration of CO_2 capture unit using blended meaamp solution into coal-fired power plants. *Energy Procedia*, *1*, 4315 – 4321. URL: http://www.sciencedirect. com/science/article/pii/S187661020900887X. doi:http://dx.doi.org/ 10.1016/j.egypro.2009.02.244. Greenhouse Gas Control Technologies 9

Proceedings of the 9th International Conference on Greenhouse Gas Control Technologies (GHGT-9), 1620 November 2008, Washington DC, USA.

Arshad, M. W., Fosbl, P. L., von Solms, N., Svendsen, H. F., & Thomsen, K. (2013). Heat of absorption of CO_2 in phase change solvents: 2-(diethylamino)ethanol and 3-(methylamino)propylamine. *Journal of Chemical & Engineering Data*, *58*, 1974–1988. URL: `http://pubs.acs.org/doi/abs/10.1021/je400289v`. `doi:10.1021/je400289v`. `arXiv:http://pubs.acs.org/doi/pdf/10.1021/je400289v`.

Cousins, A., Wardhaugh, L., & Feron, P. (2011a). A survey of process flow sheet modifications for energy efficient CO_2 capture from flue gases using chemical absorption. *International Journal of Greenhouse Gas Control*, *5*, 605 – 619. URL: `http://www.sciencedirect.com/science/article/pii/S175058361100003X`. `doi:http://dx.doi.org/10.1016/j.ijggc.2011.01.002`.

Cousins, A., Wardhaugh, L. T., & Feron, P. H. (2011b). Preliminary analysis of process flow sheet modifications for energy efficient CO_2 capture from flue gases using chemical absorption. *Chemical Engineering Research and Design*, *89*, 1237 – 1251. URL: `http://www.sciencedirect.com/science/article/pii/S0263876211000669`. `doi:http://dx.doi.org/10.1016/j.cherd.2011.02.008`. Special Issue on Distillation & Absorption.

Dugas, R., & Rochelle, G. (2009). Absorption and desorption rates of carbon dioxide with monoethanolamine and piperazine. *Energy Procedia*, *1*, 1163 – 1169. URL: `http://www.sciencedirect.com/science/article/pii/S1876610209001544`. `doi:http://dx.doi.org/10.1016/j.egypro.2009.01.153`. Greenhouse Gas Control Technologies 9 Proceedings of the 9th International Conference on Greenhouse Gas Control Technologies (GHGT-9), 1620 November 2008, Washington DC, {USA}.

Endo, T., Kajiya, Y., Nagayasu, H., Iijima, M., Ohishi, T., Tanaka, H., & Mitchell, R. (2011). Current status of mhi CO_2 cap-

ture plant technology, large scale demonstration project and road map to commercialization for coal fired flue gas application. *Energy Procedia*, *4*, 1513 – 1519. URL: http://www.sciencedirect.com/science/article/pii/S1876610211002165. doi:http://dx.doi.org/10.1016/j.egypro.2011.02.019. 10th International Conference on Greenhouse Gas Control Technologies.

Hartono, A., Saleem, F., Arshad, M. W., Usman, M., & Svendsen, H. F. (2013). Binary and ternary vle of the 2-(diethylamino)-ethanol (deea)/3-(methylamino)-propylamine (mapa)/water system. *Chemical Engineering Science*, *101*, 401 – 411. URL: http://www.sciencedirect.com/science/article/pii/S0009250913004752. doi:http://dx.doi.org/10.1016/j.ces.2013.06.052.

Hessen, E. T., Haug-Warberg, T., & Svendsen, H. F. (2010). The refined e-nrtl model applied to CO_2H_2Oalkanolamine systems. *Chemical Engineering Science*, *65*, 3638 – 3648. URL: http://www.sciencedirect.com/science/article/pii/S0009250910001582. doi:http://dx.doi.org/10.1016/j.ces.2010.03.010.

Jockenhvel, T., & Schneider, R. (2011). Towards commercial application of a second-generation post-combustion capture technology pilot plant validation of the siemens capture process and implementation of a first demonstration case. *Energy Procedia*, *4*, 1451 – 1458. URL: http://www.sciencedirect.com/science/article/pii/S1876610211002086. doi:http://dx.doi.org/10.1016/j.egypro.2011.02.011. 10th International Conference on Greenhouse Gas Control Technologies.

Just, P.-E. (2013). Advances in the development of CO_2 capture solvents. *Energy Procedia*, *37*, 314 – 324. URL: http://www.sciencedirect.com/science/article/pii/S1876610213001276. doi:http://dx.doi.org/10.1016/j.egypro.2013.05.117. GHGT-11.

Kamijo, T., Sorimachi, Y., Shimada, D., Miyamoto, O., Endo, T., Na-
gayasu, H., & Mangiaracina, A. (2013). Result of the 60 tpd CO_2
capture pilot plant in european coal power plant with KS-1$^{\text{tm}}$ sol-
vent. *Energy Procedia*, *37*, 813 – 816. URL: `http://www.sciencedirect.`
`com/science/article/pii/S1876610213001823`. doi:`http://dx.doi.org/`
`10.1016/j.egypro.2013.05.172`. GHGT-11.

Karimi, M., Hillestad, M., & Svendsen, H. F. (2011). Capital costs and energy
considerations of different alternative stripper configurations for post com-
bustion CO_2 capture. *Chemical Engineering Research and Design*, *89*, 1229
– 1236. URL: `http://www.sciencedirect.com/science/article/pii/`
`S0263876211001122`. doi:`http://dx.doi.org/10.1016/j.cherd.2011.03.`
`005`. Special Issue on Distillation & Absorption.

Kim, I., & Svendsen, H. F. (2011). Comparative study of the heats of
absorption of post-combustion CO_2 absorbents. *International Journal of*
Greenhouse Gas Control, *5*, 390 – 395. URL: `http://www.sciencedirect.`
`com/science/article/pii/S1750583610000770`. doi:`http://dx.doi.org/`
`10.1016/j.ijggc.2010.05.003`. The 5thTrondheim Conference on CO_2
Capture, Transport and Storage.

Kuettel, D. A., Fischer, B., Hohe, S., Joh, R., Kinzl, M., & Schneider, R. (2013).
Removal of acidic gases and metal ion contaminants with postcap^{TM} technol-
ogy. *Energy Procedia*, *37*, 1687 – 1695. URL: `http://www.sciencedirect.`
`com/science/article/pii/S1876610213002877`. doi:`http://dx.doi.org/`
`10.1016/j.egypro.2013.06.044`. GHGT-11.

Ma'mun, S., & Kim, I. (2013). Selection and characterization of
phase-change solvent for carbon dioxide capture: precipitating system.
Energy Procedia, *37*, 331 – 339. URL: `http://www.sciencedirect.`
`com/science/article/pii/S187661021300129X`. doi:`http://dx.doi.org/`
`10.1016/j.egypro.2013.05.119`. GHGT-11.

Ma'mun, S., Svendsen, H. F., Hoff, K. A., & Juliussen, O. (2007). Selection of new absorbents for carbon dioxide capture. *Energy Conversion and Management*, *48*, 251 – 258. URL: `http://www.sciencedirect.com/science/article/pii/S0196890406001440`. doi:`http://dx.doi.org/10.1016/j.enconman.2006.04.007`.

Moene, R., Schoon, L., van Straelen, J., & Geuzebroek, F. (2013). Precipitating carbonate process for energy efficient post-combustion CO_2 capture. *Energy Procedia*, *37*, 1881 – 1887. URL: `http://www.sciencedirect.com/science/article/pii/S1876610213003111`. doi:`http://dx.doi.org/10.1016/j.egypro.2013.06.068`. GHGT-11.

Monteiro, J. G.-S., Pinto, D. D., Zaidy, S. A., Hartono, A., & Svendsen, H. F. (2013a). Vle data and modelling of aqueous n,n-diethylethanolamine (deea) solutions. *International Journal of Greenhouse Gas Control*, *19*, 432 – 440. URL: `http://www.sciencedirect.com/science/article/pii/S175058361300354X`. doi:`http://dx.doi.org/10.1016/j.ijggc.2013.10.001`.

Monteiro, J.-S., Pinto, D., Luo, X., Knuutila, H., Hussain, S., Mba, E., Hartono, A., & Svendsen, H. (2013b). Activity-based kinetics of the reaction of carbon dioxide with aqueous amine systems. case studies: Mapa and mea. *Energy Procedia*, *37*, 1888 – 1896. URL: `http://www.sciencedirect.com/science/article/pii/S1876610213003123`. doi:`http://dx.doi.org/10.1016/j.egypro.2013.06.069`. GHGT-11.

Oyenekan, B. A., & Rochelle, G. T. (2007). Alternative stripper configurations for CO_2 capture by aqueous amines. *AIChE Journal*, *53*, 3144–3154. URL: `http://dx.doi.org/10.1002/aic.11316`. doi:`10.1002/aic.11316`.

Pinto, D. D., Monteiro, J. G.-S., Johnsen, B., Svendsen, H. F., & Knuutila, H. (2014). Density measurements and modelling of loaded and unloaded aqueous solutions of {MDEA} (n-methyldiethanolamine), {DMEA} (n,n-dimethylethanolamine), {DEEA} (diethylethanolamine) and

{MAPA} (n-methyl-1,3-diaminopropane). *International Journal of Greenhouse Gas Control*, *25*, 173 – 185. URL: http://www.sciencedirect.com/science/article/pii/S1750583614001005. doi:http://dx.doi.org/10.1016/j.ijggc.2014.04.017.

Puxty, G., Rowland, R., Allport, A., Yang, Q., Bown, M., Burns, R., Maeder, M., & Attalla, M. (2009). Carbon dioxide postcombustion capture: A novel screening study of the carbon dioxide absorption performance of 76 amines. *Environmental Science & Technology*, *43*, 6427–6433. URL: http://pubs.acs.org/doi/abs/10.1021/es901376a. doi:10.1021/es901376a. arXiv:http://pubs.acs.org/doi/pdf/10.1021/es901376a.

Raynal, L., Alix, P., Bouillon, P.-A., Gomez, A., le Febvre de Nailly, M., Jacquin, M., Kittel, J., di Lella, A., Mougin, P., & Trapy, J. (2011a). The DMX$^{\text{tm}}$ process: An original solution for lowering the cost of post-combustion carbon capture. *Energy Procedia*, *4*, 779 – 786. URL: http://www.sciencedirect.com/science/article/pii/S1876610211001214. doi:http://dx.doi.org/10.1016/j.egypro.2011.01.119. 10th International Conference on Greenhouse Gas Control Technologies.

Raynal, L., Bouillon, P.-A., Gomez, A., & Broutin, P. (2011b). From MEA to demixing solvents and future steps, a roadmap for lowering the cost of post-combustion carbon capture. *Chemical Engineering Journal*, *171*, 742 – 752. URL: http://www.sciencedirect.com/science/article/pii/S1385894711000350. doi:http://dx.doi.org/10.1016/j.cej.2011.01.008. Special Section: Symposium on Post-Combustion Carbon Dioxide Capture.

Razi, N., Svendsen, H. F., & Bolland, O. (2013). Cost and energy sensitivity analysis of absorber design in CO_2 capture with MEA. *International Journal of Greenhouse Gas Control*, *19*, 331 – 339. URL: http://www.sciencedirect.com/science/article/pii/

S1750583613003411. doi:http://dx.doi.org/10.1016/j.ijggc.2013.09.008.

Rey, A., Gouedard, C., Ledirac, N., Cohen, M., Dugay, J., Vial, J., Pichon, V., Bertomeu, L., Picq, D., Bontemps, D., Chopin, F., & Carrette, P.-L. (2013). Amine degradation in CO_2 capture. 2. new degradation products of /mboxMEA. pyrazine and alkylpyrazines: Analysis, mechanism of formation and toxicity. *International Journal of Greenhouse Gas Control*, *19*, 576 – 583. URL: http://www.sciencedirect.com/science/article/pii/S175058361300371X. doi:http://dx.doi.org/10.1016/j.ijggc.2013.10.018.

Rochelle, G., Chen, E., Freeman, S., Wagener, D. V., Xu, Q., & Voice, A. (2011). Aqueous piperazine as the new standard for CO_2 capture technology. *Chemical Engineering Journal*, *171*, 725 – 733. URL: http://www.sciencedirect.com/science/article/pii/S1385894711001793. doi:http://dx.doi.org/10.1016/j.cej.2011.02.011. Special Section: Symposium on Post-Combustion Carbon Dioxide Capture.

Sanchez-Fernandez, E., de Miguel Mercader, F., Misiak, K., van der Ham, L., Linders, M., & Goetheer, E. (2013). New process concepts for CO_2 capture based on precipitating amino acids. *Energy Procedia*, *37*, 1160 – 1171. URL: http://www.sciencedirect.com/science/article/pii/S1876610213002233. doi:http://dx.doi.org/10.1016/j.egypro.2013.05.213. GHGT-11.

Shaw, D. (2009). Cansolv CO_2 capture: The value of integration. *Energy Procedia*, *1*, 237 – 246. URL: http://www.sciencedirect.com/science/article/pii/S1876610209000356. doi:http://dx.doi.org/10.1016/j.egypro.2009.01.034. Greenhouse Gas Control Technologies 9 Proceedings of the 9th International Conference on Greenhouse Gas Control Technologies (GHGT-9), 1620 November 2008, Washington DC, {USA}.

Svendsen, H., & Trollebø, A. (2013). An amine absorbent and a method for CO_2

capture. URL: `http://www.google.com/patents/WO2013000953A2?cl=en` wO Patent App. PCT/EP2012/062,463.

Svendsen, H. F., Hessen, E. T., & Mejdell, T. (2011). Carbon dioxide capture by absorption, challenges and possibilities. *Chemical Engineering Journal*, *171*, 718 – 724. URL: `http://www.sciencedirect.com/science/article/pii/S1385894711000416`. doi:`http://dx.doi.org/10.1016/j.cej.2011.01.014`. Special Section: Symposium on Post-Combustion Carbon Dioxide Capture.

Vevelstad, S. J., Grimstvedt, A., Elnan, J., da Silva, E. F., & Svendsen, H. F. (2013). Oxidative degradation of 2-ethanolamine: The effect of oxygen concentration and temperature on product formation. *International Journal of Greenhouse Gas Control*, *18*, 88 – 100. URL: `http://www.sciencedirect.com/science/article/pii/S1750583613002569`. doi:`http://dx.doi.org/10.1016/j.ijggc.2013.06.008`.

Voice, A. K., Vevelstad, S. J., Chen, X., Nguyen, T., & Rochelle, G. T. (2013). Aqueous 3-(methylamino)propylamine for CO_2 capture. *International Journal of Greenhouse Gas Control*, *15*, 70 – 77. URL: `http://www.sciencedirect.com/science/article/pii/S1750583613000765`. doi:`http://dx.doi.org/10.1016/j.ijggc.2013.01.045`.